This document is downloaded from DR-NTU (https://dr.ntu.edu.sg)
Nanyang Technological University, Singapore.

Protein expression profiles in osteoblasts in response to differentially shaped hydroxyapatite nanoparticles

Xu, Jinling; Khor, Khiam Aik; Sui, Jianjun; Zhang, Jianhua; Chen, William Wei Ning

2009

Xu, J., Khor, K. A., Sui, J., Zhang, J., & Chen, W. N. W. (2009). Protein expression profiles in osteoblasts in response to differentially shaped hydroxyapatite nanoparticles. Biomaterials, 30(29), 5385-5391.

https://hdl.handle.net/10356/95665

https://doi.org/10.1016/j.biomaterials.2009.07.002

©2009 Elsevier Ltd. This is the author created version of a work that has been peer reviewed and accepted for publication by Biomaterials, Elsevier Ltd. It incorporates referee’ s comments but changes resulting from the publishing process, such as copyediting, structural formatting, may not be reflected in this document. The published version is available at: DOI [http://dx.doi.org/10.1016/j.biomaterials.2009.07.002].

Downloaded on 13 Mar 2024 18:42:53 SGT

Protein Expression Profiles in Osteoblasts in Response to Differentially Shaped Hydroxyapatite Nanoparticles

Jinling Xu[†, 1], Khiam Aik Khor[1], Jianjun Sui[2], Jianhua Zhang[2], Wei Ning Chen[†, 2]

[1]School of Mechanical & Aerospace Engineering,

[2]School of Chemical and Biomedical Engineering

Nanyang Technological University, 50 Nanyang Avenue, Singapore 639798

Abstract

The use of synthetic hydroxyapatite as bone substitute calls for the knowledge of the influence on adjacent cells. The aim of this study was to investigate the proteins with differential protein expression levels in the proteome of human osteoblast cell line incubated separately with various nano sized hydroxyapatite powders with different shapes and chemical compositions using iTRAQ coupled 2D LC MS/MS approach. In the present study, we investigated several intracellular signaling molecules involved in calcium regulation to analyze how osteoblast cells respond to dissimilar HA nanoparticles. It was found there was a significant decrease in cell population after adding the HA nanoparticles to the osteoblasts. Our results combining proteomics analysis and RT-PCR validation on targeted genes involved in calcium regulation confirmed the differences in the cellular response to dissimilar HA nanoparticles.

Keywords: nanoparticles, hydroxyapatite, osteoblast, iTRAQ, protein profile, LC-MS/MS analysis

1. Introduction

The majority of bone consists of extracellular matrix proteins and the mineral hydroxyapatite (HA). HA has been well characterized chemically and mechanically as its benefits are demonstrated in both short- and long-term clinical results [1-5]. It does not induce local or systemic toxicity, inflammation, or foreign body response, or intervening fibrous tissue between implant and bone. The biocompatibility of HA have evaluated with the use of simple immersion tests in simulated body fluids with ionic concentration, showing that formation of apatite deposition on the surface of the material immersed in the fluid. The precipitated apatite layer is desirable to result in the formation bond between bone and materials. However, it also should consider carefully about the loosening HA particles production and accumulation from the prosthetic implants which limits the longevity of prosthesis [6, 7]. Aseptic loosening after total joint arthroplasty is a major problem in orthopedic surgery. It is due to an osteolysis resulting from oasteoclast activation by the cytokines and growth factors synthesized by the macrophages which phagocytosed the wear debris [1, 8]. It has been also documented numerously that the use of synthetic HA as bone substitute has called for the influence on the adjacent cells *in vitro* [8-11]. Interactions of bone cells with HA surfaces are mediated by adhesion receptors belonging to the integrin family. Many papers dealt with the synthesis of nano-structured HA, currently one of the most demanding challenges for producing new biomaterials [2-5]. Calcium ions and phosphate ions are essential materials for cell mineralization and suitable concentrations of calcium and inorganic phosphates in culture media would maintain and/or enhance cell growth and proliferation. However, the release of particles during the resorption of HA based

[†] Corresponding author Tel: 65 6790 6875 E-mail:jlxu@ntu.edu.sg and wnchen@ntu.edu.sg

materials has been a cause of concern. The interactions between HA particles and human monocytes leads to the release of inflammatory mediators [1]. The present report aims to use proteomics analysis to establish protein profile in osteoblast cells in response to HA, which in turn should provide helpful information on the possible injurious effects of nano sized HA powder to osteoblasts. To validate our findings, the expression of several marker genes was analyzed further by RT-PCR. The potential implications on future design of bone substitutes were also discussed.

2. Experimental

2.1 Nanoparticles preparation

The HA nanoparticles used in this study were prepared according to a previous study [12]. Briefly, the needle shape HA nanoparticles with phase pure HA was obtained by a precipitation methods using the chemical reaction of $Ca(OH)_2$ and H_3PO_4 by adjusting the pH to 9. The spherical HA based nanoparticles (spherical HA nanoparticles) was synthesized using a radio frequency plasma at the working power level of 20 kW. The powder morphologies were characterized with a field emission scanning electron microscope (FE SEM, JEOL 6340F).

2.2 Cell culture

Osteoblasts from a cell line of hFOB 1.19 (ATCC, CRL-11372) were seeded with an initial cell density of 5×10^4 /cm^2 with dissimilar HA nanoparticles at a concentration of 10 mg/ml and incubated at 37 °C in a 5% CO_2 atmosphere. The culture medium used for each sample was 10 ml of Dulbecco's modified Eagle's medium/F12 supplemented with 10 volume% of fetal bone bovine serum and 5 volume % of antibiotics. To determine the cell densities after culturing, the osteoblasts were detached by trypsinization and counted in a haemocytometer under an optical microscope.

2.3 Cell Lysis, Protein Digestion, and Labeling with iTRAQ Reagents

100 µg of protein samples were collected from the cells after exposure to nanoparticles for 4 days according to the previous study [9]. After denatured and cysteins blocked as described in the iTRAQ protocol (Applied Biosystems), each sample was then digested with 20 µl of 0.25 µg/ µl sequence grade modified trypsin (Promega, USA) solution at 37 °C overnight. The samples were labeled with the iTRAQ tags as follows: control group, iTRAQ 114; needle shape phase pure HA nanoparticles, iTRAQ 115; RF plasma prepared spherical nanoparticles, iTRAQ 116. All experiments were carried out in three independent runs.

2.4 Data Analysis and Interpretation

Peptide identifications were performed using ProID software packages (Applied Biosystems). The analysis for the iTRAQ experiments was performed with ProQUANT 1.0. The cut off for the confidence settings was 75 and the tolerance setting for peptide identification in ProQUANT searches were 0.15 Da for MS and 0.1 Da for MS/MS. ProQUANT pooled data from all the series of runs of increasing concentration of KCl in one experiment. All identifications were manually inspected for correctness. Relative quantification of proteins in the case of iTRAQ is performed on the MS/MS scans and is the ratio of the areas under the peaks at 114, 115, and 116 Da which are the masses of the tags that correspond to the iTRAQ reagents. The relative amount of a peptide in each sample was calculated by dividing the peak areas observed at 115.1, and 116.1 m/z by that observed at 114.1 m/z.

2.5 Real-time reverse transcriptase-polymerase chain reaction (RT-PCR)

Total RNA was extracted from osteoblast cells in the presence of soluble nano HA powders at the initial culturing stage of 4 days using RNeasy mini kit (Qiagen) as described [13]. The flow-out RNA sample after centrifuged was added DNase to remove genomic DNA contamination. The quantization of RNA was determined by measuring the absorbance at 260 nm (A_{260}) in a spectrophotometer. To accurately quantify the original amount of target mRNAs in samples, Real-time RT-PCR was applied using iSCRIPT one-step RT-PCR kit (Bio-Rad) as described [13]. The real-time PCR was carried out in an IQ 5 multicolor Real-time PCR detection system (Bio-Rad). The cycling program was: 50^{o}C for 10 min, 95 ^{o}C 5min; repeat 40 times the following: 95 ^{o}C 10 sec, 60 ^{o}C 30 sec. The disassociation analysis was routinely carried out by acquiring fluorescent reading for one degree increase from 55 ^{o}C to 95 ^{o}C. Microsoft Excel formatted data including amplification analysis, experimental report, melting curve analysis and threshold cycle number were provided automatically by IQ5 optical system software version 2.0 (Bio-Rad). The fold changes were calculated as following formula:

Sample Δ**Ct=Ct $_{\text{sample}}$-Ct $_{\beta\text{-actin}}$;**

$\Delta\Delta$Ct= **Sample ΔCt-control ΔCt;**

the fold of sample VS control = $2^{-\Delta\Delta Ct}$.

PCR primers were carefully designed to give a product around 150-200 base pairs to reduce the nonspecific binding of SYBR Green. Actin primers were used as internal controls along with the primers of gene being analyzed. The primers sequences were shown below:

5'-ACTCGTCCCTGATTGCTGTTA-3'(the sense primer for calgizzarin);

5'-ACTGGGGTCTGGTTCCTTGTG-3' (the anti sense primer for calgizzarin);

5'-AATCTGACCCGGTCGTCTCGT-3' (the sense primer for elongation factor 2);

5'-GCGGACACCTCGCCTTTATCG-3' (the anti sense primer for elongation factor 2);

5'- AGCCACCGAGACACCATGAGA-3' (the sense primer for osteocalcin);

5'-GCAAAGGGACTGCCAGCCAAA-3' (the anti sense for osteocalcin);

5'-CTGGTGGAAGGAGGCAGAATT-3' (the sense primer for alkaline phosphatase, AKP);

5'-ATGTGAAGACGTGGGAATGGT-3' (the anti sense primer for alkaline phosphatase);

5′-GGTCCAGTCTAGACACTCTTCG-3′ (the sense primer for thioredoxin);

5′-CCCACAAGCTTGTCGACTTCC-3′ (the anti sense primer for thioredoxin);

5'-CTTAGTTGCGTTACACCCTTTC-3' (the sense primer for human beta-actin);

5'-ACCTTCACCGTTCCAGTTTT-3' (the anti sense primer for human beta-actin).

2.6 Intracellular Ca^{2+} Concentration Measurements

A Fluo-4 NW Calcium Assay kit (Invitrogen) was used to measure intracellular Ca^{2+} concentration on a fluorometer (Tecan) following the manufacturer's protocols. Briefly, each of the cells in the presence of dissimilar HA nanoparticles was cultured separately in a 96-well plate. The growth medium was replaced with 100 µL/well Fluo-4 dye solution containing probenecid to prevent extrusion of the dye out of cells. The plate was maintained at 37 °C for 30 min and then at room temperature for an additional 30 min. The assay was done at 494 nm for excitation and at 516 nm for emission.

2.7 Statistics

The data shown are representative of three to four separate experiments performed in duplicate, and values are expressed as means ± SD (standard deviation). The differences between various HA nanoparticles were evaluated by ANOVA. The level of statistical significance was defined as $p<0.05$.

3. Results and Discussion

To investigate possible injurious effects of nano sized HA powder to osteoblasts, two types of nano sized HA particles (needle shape and spherical shape) were prepared. Figure 1 showed the distinct FE SEM morphologies of the nano HA particles prepared for this study. While needle shaped nano HA particles showed a width of 10-15 nm and length of 80-100nm, the spherical nano HA particles displayed a wide particle size distribution in the range of 10-100 nm including amorphous phase, HA, alpha tricalcium phosphate and CaO [12].

Nano-sized HA may lead to higher Ca^{2+} concentration of culture media compared with its conventional counterpart [14]. An elevated concentration of calcium, resulting from direct addition of Ca^{2+} ion sources or dissolution of HA nanoparticles, has been shown to lead to decreased proliferation and/or osteogenic differentiation of mesenchymal stem cells [14]. Cell density measurement in the presence of the two types of nano HA particles was carried out. Results shown in Figure 2 indicated that direct addition of HA nanoparticles to osteoblast cultures significantly affected the cell counts compared to the possible positive effect of Ca^{2+} ions in the media. The cell populations in the presence of HA particles were significantly lower than those of control groups at both of 2 and 4 culturing days. The cell counts on the culturing for 4 days between the needle shaped HA nanoparticles and spherical HA nanoparticles showed some significant difference. This could be due to the high dissolution possibility of secondary calcium phosphates in spherical nanoparticles which resulted in the decreased cell exposure to the surfaces of nanoparticles thus leading to moderate toxicity. Our findings suggested that the decrease in cell number after exposure to the test material may be used as a marker for the toxicity of the tested materials.

Proteome analysis has proven to be an effective approach to comprehensive analysis of the regulatory network of differentiation. The information generated from such an analysis could in turn help in the design of better biomaterials in term of improved biocompatibility. To establish a global protein profile in osteoblasts in response to a particular type of nano HA particles, the 2D iTRAQ-coupled LC-MS/MS analysis was used in this study. Results from three independent runs revealed 37 proteins with unused protein score more than 99% confidence with unique peptide contribution value >2.0 and the fold difference is greater than 1.20 or less than 0.80. According to their cellular functions, these proteins were subsequently categorized into three groups: cytoskeletal proteins (Table 1), metabolic enzymes (Table 2) and cell growth proteins (Table 3). In addition, peptide sequences of these identified proteins was included in Table 4.

As listed in Table 1, the osteoblasts in response to HA nanoparticles showed obvious different regulations in the cytoskeletal proteins expression levels. Generally, most of cytoskeletal proteins in the osteoblasts exposed to the needle shaped HA particles showed protein expression levels similar to those cultured on the polystyrene with the fold difference less than 0.2. However, the proteins which are major structural proteins of cytoskeleton (actin, vimentin and tubulin) in cells exposed to the spherical nanoparticles showed a fold changes (either up- or down-regulation) greater than 0.2. Proteins found to be up-regulated in cells exposed to spherical nano HA particles included vimentin, actin, tubulin, ezrin, myosin and transgelin. On the other hand, proteins found to be down-regulated in cells exposed to spherical nano HA particles included filamin-A, filamin-B and talin (Table 1). As these proteins play a critical role in cell architecture/mobility, the changes in the level of these cytoskeletal modulations may suggest cellular response to mechanical strain within osteoblasts [15].

Interestingly, an increased talin binding to integrin has been shown to lead to stronger cell adhesion, thus less cell migration [16]. Similarly, increased filamin binding to integrin receptor has been associated with an inhibition of cell migration [21]. Since the decreased level in both talin and filamin was observed in osteoblasts exposed to spherical nano HA particles, our data suggested an increase in cell migration in these cells as compared with those exposed to needle shaped nano HA particles. Our result may indicate that the signal transduction from the external environment into the intracellular domain has brought about structural changes to cells. This transduction may occur through different biochemical pathways including the activation of a wide variety of intracellular second messages such as calcium-mediated cell signaling pathways. Another cytoskeletal protein, transgelin, also showed significant up-regulation in cells exposed to spherical nano HA particles (Table 1). Transgelin has been shown to bind to actin *in vitro* and modulate a variety of physiological processes including motility of cells by interacting differently with the actin cytoskeleton. Similarly to a recent report, the upregulation of transgelin in our study may point to the increased motility of osteoblasts exposed to spherical nano HA particles [22]. Taken together, the changes of protein levels in osteoblasts exposed to spherical nano HA particles suggested an increase in the migration of these cells.

As shown in Table 2, most of the metabolic enzymes involved in the pathways of glycolysis and oxidative phosphorylation (except the glycolytic enzyme Glucose-6-phosphate isomerase) showed relatively higher up-regulation levels in cells exposed to either needle shape or spherical HA nanoparticles as compared to those in control group. The assessment of glycolytic activity of osteoblasts is not a standard tool in most of the reports, but might be of value by providing a direct indicator of cellular metabolism. Enzymes involved in glycolysis and adenosine triphosphate (ATP) biosysnthesis were generally reported as markers of the energy-demanding differentiation. Their over-expression was associated to an accelerated glycolysis rate which is expected to affect the cellular energy metabolism and consequently influences the oxidative phosphorylation rates, increasing ATP levels.

In addition, as shown in Table 2, the levels of thioredoxin (Trx) acting as antioxidants in the cells response to HA nanoparticles showed significant up-regulation as compared to those in control group (over 2 fold for osteoblasts exposed to either the needle-shaped or spherical HA nanoparticles). Thiroredoxins are low molecular weight (10-12 Kda) proteins with oxidoreductase activity. One of Trx functions is regulation of apoptosis which is a form of programmed cell death. It is clear that the antioxidant Trx system is regarded as a tumor-preventing system. This applies not only to the detoxification of reactive oxygen metabolites but also to signaling processes. Our result indicated the presence of high content of oxidative stresses in the cells exposure to HA nanoparticles. The oxidative stress is considered as a key factor for DNA damage, which particularly explains that the decrease in cell population after exposure to the test nanoparticles through a series of biochemical events leading to a characteristic cell death [17]. In addition, considering the relatively higher expressions in the metabolic enzymes, the complexity of chemical components in the spherical nanoparticles may be more potentially hazardous to the osteoblasts when compared to such exposure to the needle shape particles.

Table 3 listed the differentially expressed signaling and cell growth proteins in the osteoblasts. Interactions of bone cells with HA surfaces are mediated by adhesion receptors belonging to the integrin superfamily that recognize binding domains within proteins of the extracellular matrix. Integrin-mediated adhesion to extracellular proteins activates multiple cytoskeletal-associated and intracellular signaling proteins. In the present study, we investigated several intracellular signaling molecules involved in calcium regulation to analyze how osteoblast cells respond to dissimilar shaped HA nanoparticles. Two S100 calcium binding proteins, calpactin and calgizarrin, showed obvious up-regulation in expression. S100 proteins are involved in regulation of protein phosphorylation, transcription factors, Ca^{2+} homeostasis, the dynamics of cytoskeleton constituents,

enzyme activities, cell growth and differentiation, and the inflammatory response. Calpactin is a protein providing a link between membrane lipids and the cytoskeleton. Calgizarrin is localized in the cytoplasm in resting cells and moves to the cell periphery in culture epidermal keratinocytes following calcium challenge. This movement requires the presence of intact microtubules. Ca^{2+} binding to calgizarrin induces a conformational change that exposes a hydrophobic surface for interaction with target proteins [18]. Elongation factor-2 is absolutely dependent on the concentration of Ca^{2+} for activity. In addition, another Ras-related GTP-binding protein which was identified as HA-inducible gene [19] also showed an obvious upregulation with 1.5 fold expression change in response to spherical HA nanoparticles. Taken together, these observations suggest that the signals from HA may modulate several proteins involved with Ca^{2+}. The addition of HA nanoparticles with a concentration of 10 mg/ml (~0.1mM) could not greatly affect the culture media ion concentrations but microenvironment around the nanoparticles. This could influence the intracellular calcium ions in the cells live with nanoparticles. Quantification of the ratio of intracellular Ca^{2+} concentration in the osteoblast cells after culturing for 4 days in respond to HA nanoparticles showed about 90.6% in HA nanoparticles and 84.8% in spherical HA nanoparticles as compared to the readings of control group (data not shown). Calcium itself is a modulator of intracellular events. The various chemical components inclusive of HA, amorphous calcium phosphate tricalcium phosphate from spherical particles may modify several signaling pathways related with Ca^{2+} and therefore have significantly influenced the osteoblast cells activities. The local fluctuations in Ca^{2+} may regulate osteoblast activity during both Ca^{2+} load buffering by bone, where the cells are exposed to large increases in Ca^{2+}, and remodeling, when the local elevations in Ca^{2+} are more moderate. The changes of calcium ion concentrations of the microenvironment in which the osteoblasts live can affect the biological behavior of the seeded in many ways [14]. The mechanisms involved are still unknown.

Analysis of steady-state mRNA levels for calgizzarin, elongation factor-2 and thioredoxin as well as the classical markers of osteoblast differentiation, such as osteocalcin and alkaline phosphatase, was carried out to determine whether changes that were observed in the synthetic and accumulated levels of the various proteins were regulated at a transcriptional level. The levels of the cytoskeletal actin mRNA expression were assessed as a control because these proteins did not change in response to the various exposures to nanoparticles. In this study, we did not expect any obvious side effects resulting from the various shaped HA nanoparticles but keep the normal osteoblasts behaviors as those cultured on the Petri dish. As shown in Figure 3, the analysis demonstrated that the calgizzarin mRNA that encoded for protein showing changes in its accumulation and synthesis also changed in its mRNA expression level. In contrast, the expression of cytoskeletal actin mRNA remained constant. The discrepancy between proteomics and PCR might be sensitivity between two analysis methods. Actually, there is no quantitative correlation between mRNA and corresponding protein levels [20]. As shown in Figure 3, the mRNA levels of elongation factor-2 and thioredoxin from the cells exposure to needle shaped HA nanoparticles showed the gene expression changes were more than 2-fold. The elongation factor-2 kinase is a negative regulator of eukaryotic mRNA translation. This result showed that the rate of peptide chain elongation was increased in the cells exposure to the needle shape nanoparticles but reduced in those osteoblasts exposure to spherical particles, indicating that the different solubility of various calcium phosphates phases in the spherical particles may influence the signal transduction pathways related with calcium regulation.

Osteocalcin is one of the major non-collagenous proteins incorporated in bone matrix during bone formation. On the other hand, the alkaline phosphatase (AKP) also plays an important role in the early stage of cell proliferation. The mRNA levels for osteocalcin and AKP increased relatively high in the cells cultured with the presence of phase pure needle-shaped HA nanoparticles, suggesting that HA enhances osteoblast differentiation, a useful characteristics for developing an optimum bone-implant scaffold. However, the spherical particles showed a relatively decrease in the expression of these differentiation markers. As suggested by Liu et al [14], the variation phosphate concentration

from the nanoparticles may have no effect on the cell differentiation. However, the complexity of chemical composition (inclusive of HA, TCP, CaO and even amorphous phase) in the spherical nanoparticles resulting in the greater degree of Ca^{2+} ion release should have significantly influenced affected the cellular responses by possibly inhibiting the mRNA expression levels as compared to those cells cultured in the presence of needle shaped HA nanoparticles. In addition, the particle shape can also contribute modulation of osteoblast gene expression. The potentially interesting hypothesis is that differences in particle shape, leads to altered surface characteristics that are sensed by osteoblasts.

4. Summary

This study demonstrated that HA based nanoparticles showed inhibitory effects on osteoblasts by decreasing the cell populations at the initial culturing stage. The various profiled proteins and genes expression levels in the osteoblasts were detected in response to the different HA nanoparticles, suggesting that the chemical components may greatly affect the osteoblast cell activities. Thus special consideration should be noted to the potential hazards of smaller HA particles degraded from the HA based materials supplied for clinical use.

Acknowledgements

We would like to thank Academic Research Funds, Ministry of Education, Singapore, for funding support. J.L. Xu is a research fellow in School of Mechanical & Aerospace Engineering, Nanyang Technological University. J.J. Sui is recipient of graduate scholarship from Nanyang Technological University. J.H. Zhang is recipient of Singapore Millennium Foundation scholarship.

References

[1]. Grandjean-Laquerriere A, Tabary O, Jacquot J, Richard D, Frayssinet P, Guenounou M, Laurent-Maquin D, Laquerrier P, Gangloff S. Involvement of toll-like receptor 4 in the inflammatory reaction induced by hydroxyapatite particles. Biomater 2007; 28: 400-404.

[2]. Xie J, Baumann MJ, McCabe LR. Osteoblasts respond to hydroxyapatite surfaces with immediate changes in gene expression. J Biomed Mater Res A 2004;71:108-117.

[3]. Hott M, Noel B, Didier BA, Rey C, Marie PJ. Proliferation and differentiation of human trabecular osteoblastic cells on hydroxyapatite. J Biomed Mater Res 1997;37:508-516.

[4]. Annaz B, Hing KA, Kayser M, Buckland T, Disilvio L. Porosity variation in hydroxyapatite and osteoblast morphology: a scanning electron microscopy study. J Micro 2004, 215, p100-110.

[5]. Redey SA, Nardin M, Assolant DB, Rey C, Delannoy P, Sedel L, et al. Behavior of human osteoblastic cells on stoichiometric hydroxyapatite and type A carbonate apatite: Role of surface energy. J Biomed Mater Res 2000;50:353-364.

[6]. Shu R, McMullen R, Baumann MJ, McCabe LR. Hydroxyapatite accelerates differentiation and suppresses growth of MC3T3-E1 osteoblasts; J Biomed Mater Res A 2003;67:1196-1204.

[7]. Sun JS, Liu HC, Chang, WHS, Li J, Lin FH, Tai HC. Influence of hydroxyapatite particle size on bone cell activities: an in vitro study; J Biomed Mater Res 1998;39:390-397.

[8]. Bloebaum RD, DuPont JA. Osteolysis from press-fit hydroxyapatite coated implant. J Arthroplasty 1993;8:195-202.

[9]. Xu JL, Khor KA, Sui JJ, Zhang JH, Tan TL, Chen WN. Comparative Proteomics Profile of Osteoblasts Cultured on Dissimilar Hydroxyapatite Biomaterials: An iTRAQ-coupled 2D LC-MS/MS Analysis. Proteom 2008;8:4249-4258

[10]. Lu YP, Chen YM, Li ST, Wang JH. Surface nanocrytallinzation of hydroxyapatite coating. Acta Biomater 2008;4:1865-1872.

[11]. Sun JS, Lin FH, Hung TY, Tsuang YH, Chang WHS, Liu HC. The influence of hydroxyapatite particles on osteoclast cell activities. J Biomed Mater Res 1999;45:311- 321.

[12]. Xu JL, Khor KA, Dong ZL, Gu YW, Kumar R, Cheang P. Preparation and characterization of nano-sized hydroxyapatite powders produced in a radio frequency (rf) thermal plasma. Mater Sci Eng A 2004;374:101-108.

[13]. Zhang JH, Sui JJ, Ching CB, Chen WN. Protein profile in neuroblastoma cells incubated with *S*- and *R*-enantiomers of ibuprofen by iTRAQ-coupled 2D LC-MS/MS analysis: possible action of induced proteins on Alzheimer's disease. Proteom 2008;8:1595-1607.

[14]. Liu YK, Lu QZ, Pei R, Ji HJ, Zhou GS, Zhao XL, Tang RK, Zhang M. The effect of extracellular calcium and inorganic phosphate on the growth and osteogenic differentiation of mesenchymal stem cells in vitro: implication for bone tissue engineering. Biomed Mater 2009; 4: 025004(8pp).

[15]. Meazzini MC, Toma CD, Schaffer JL, Gray ML, Gerstenfeld LC. Osteoblast cytoskeletal modulation in response to mechanical strain in vitro; J Orthop Res 1998;6:170-180.

[16]. Li YF, Tang RH, Puan KJ, Law SK, Tan SM. The cytosolic protein talin induces an intermediate affinity integrin alphaLbeta2. J Biol Chem. 2007:282:24310-9.

[17]. Drew JE, Padidar S, Horgan G, Duthie GG, Russell WR, Reid M, et al. Salicylate modulates oxidative stress in the rat colon: A proteomic approach. Biochemical Pharmacology 2006;72:204-216.

[18]. Mannan AU, Nica G, Nayernia K, Mueller C, Engel W. Calgizarrin like gene (Cal) deficient mic undergo normal spermatogenesis. Molecul Reproduct Develop 2003;66:431-438.

[19]. Song JH, Kim JH, Park S, Kang W, Kim HW, Kim HE, et al. Signaling response of osteoblast cells to hydroxyapatite: the activation of ERK and SOX9. J Bone Miner Metab 2008;26:138-142.

[20]. Gygi SP, Rochon Y, Franza BR, Bebersold R. Correlation between protein and mRNA abundance in Yeast. Molecular Cellular Biology 1999;19:1720-1730.

[21]. Calderwood DA, Huttenlocher A, Kiosses WB, Rose DM, Woodside DG, Schwartz MA, Ginsberg MH. Increased filamin binding to beta-integrin cytoplasmic domains inhibits cell migration. Nat Cell Biol 2001:3:1060-8.

[22]. Zhang R, Zhou L, Li Q, Liu J, Yao W, Wan H. Upregulation of Two Actin Associated Proteins Prompts Pulmonary Artery Smooth Muscle Cell Migration Under Hypoxia. Am J Respir Cell Mol Biol. 2009 Feb 2

List of Tables

Table 1 List of different expressed cytoskeletal proteins in osteoblast cells (115/114 and 116/114 are the ratios of different protein expression level in the cells culture in respond to needle shape HA and spherical HA nanoparticles, respectively. SD: standard deviation)

Table 2 List of differentially expressed Metabolic Enzymes in osteoblasts (115/114 and 116/114 are the ratios of different protein expression level in the cells culture in respond to needle shape HA and spherical HA nanoparticles, respectively.)

Table 3 List of differentially expressed Signaling and cell growth proteins in osteoblasts (115/114 and 116/114 are the ratios of different protein expression level in the cells culture in respond to needle shape HA and spherical HA nanoparticles, respectively.)

Table 4 List of peptide sequences of identified proteins

List of Figures

Figure 1 FE SEM images of (a) needle-shaped HA nanoparticles and (b) spherical HA nanoparticles.

Figure 2 Cell densities of osteoblasts when cultured with dissimilar shaped HA nanoparticles at a concentration of 1 mg/ml. The initial cell density is $2x10^5/cm^2$.

Figure 3 Various mRNA expression changes in respond to needle shape HA and spherical HA nanoparticles ($p<0.05$).

Proteins name	Cellular function	115/114 ±SD	116/114 ±SD
Vimentin	Cytoskeleton and internal cell motility	1.08±0.08	1.25±0.09
Actin, cytoplasmic 2 (Gamma-actin)	Cytoskeleton and internal cell motility	1.13±0.12	1.37±0.06
Tubulin alpha-6 chain	Cytoskeleton and internal cell motility	1.07±0.09	1.29±0.10
Filamin-A	Cytoskeleton and internal cell motility	0.96±0.45	0.73±0.17
Talin-1	Cytoskeleton and internal cell motility	0.97±0.32	0.72±0.26
Ezrin (p81) (Cytovillin)	Cytoskeleton and internal cell motility	1.08±0.10	1.30±0.11
Ubiquitin	Cytoskeleton and internal cell motility	1.13±0.17	1.29±0.08
Myosin light polypeptide 6	Cytoskeleton and internal cell motility	0.97±0.15	1.25±0.13
Filamin-B	Cytoskeleton and internal cell motility	0.88±0.25	0.72±0.19
Transgelin	Cytoskeleton and internal cell motility	0.92±0.32	1.34±0.53

Table 1

Proteins names	Cellular function	115/114 ±SD	116/114 ±SD
Glyceraldehyde-3-phosphate dehydrogenase	Glycolysis	1.04±0.05	1.22±0.03
Pyruvate kinase isozymes	Glycolysis	1.13±0.02	1.23±0.03
Peptidyl-prolyl cis-trans isomerase A	Dephosphorylation	1.02±0.20	1.28±0.18
Fructose-bisphosphate aldolase A	Glycolysis	1.06±0.14	1.30±0.14
ADP/ATP translocase 1	Energy transfer	1.24±0.13	1.28±0.12
Glucose-6-phosphate isomerase	Glycolysis	0.92±0.02	0.75±0.01
Protein disulfide-isomerase precursor	Protein folding and chaperone	1.03±0.46	0.69±0.19
Thioredoxin	Oxidoreductase	2.18±0.15	2.99±0.14

Table 2

Proteins names	Cellular function	115/114 ±SD	116/114 ±SD
Annexin A2 (Annexin II) (Lipocortin II) (Calpactin I heavy chain)	Cell-matrix interaction	1.08±0.02	1.20±0.01
Histone H2B type F-S (H2B.s) (H2B/s)	Chromatin assembly	1.05±0.06	1.22±0.03
Histone H3.1	Chromatin assembly	1.01±0.15	0.63±0.18
Heterogeneous nuclear ribonucleoproteins A2/B1	Protein translation	1.11±0.17	1.53±0.18
Eukaryotic translation initiation factor 5A-1	Protein translation	1.18±0.10	1.28±0.10
Calgizzarin	Cell-matrix interaction	1.50±0.18	1.49±0.21
Eukaryotic translation initiation factor 2C 4	Protein translation	0.93±0.30	0.51±0.31
Elongation factor 2	Protein translation	1.55±0.12	1.23±0.09
Chloride intracellular channel protein 1	Cell-matrix interaction	1.12±0.12	1.45±0.12
NHP2-like protein 1 (High mobility group-like nuclear protein 2 homolog 1)	protein biosynthesis	1.46±0.24	1.28±0.15
40S ribosomal protein S12	Protein translation	1.19±0.19	1.28±0.30
Ras-related protein Rap-1b precursor (GTP-binding protein smg p21B)	Hydrolysis	1.14±0.23	1.53±0.22

Table 3

ProtSc	Accession	Contrib	Conf	Sequence
Vimentin				
37.23	P08670	2	99	DNLAEDIMR
37.23	P08670	2	99	EEAENTLQSFR
37.23	P08670	2	99	EMEENFAVEAANYQDTIGR
37.23	P08670	2	99	ETNLDSLPLVDTHSK
37.23	P08670	2	99	FADLSEAANR
37.23	P08670	2	99	ILLAELEQLK
37.23	P08670	2	99	ILLAELEQLKGQGK
37.23	P08670	2	99	ISLPLPNFSSLNLR
37.23	P08670	2	99	KVESLQEEIAFLK
37.23	P08670	2	99	QVQSLTCEVDALK
37.23	P08670	2	99	SLGSALRPSTSR
37.23	P08670	2	99	SLYASSPGGVYATR
37.23	P08670	2	99	TYSLGSALRPSTSR
37.23	P08670	2	99	VELQELNDR
Actin, cytoplasmic 2 (γ-actin)				
27.52	P60709	2	99	AVFPSIVGR
27.52	P60709	2	99	AVFPSIVGRPR
27.52	P60709	2	99	DLYANTVLSGGTTMYPGIADR
27.52	P60709	2	99	EITALAPSTMK
27.52	P60709	2	99	GYSFTTTAER
27.52	P60709	2	99	LCYVALDFEQEMATAASSSSLEK
27.52	P60709	2	99	MTQIMFETFNTPAMYVAIQAVLSLYASGR
27.52	P60709	2	99	QEYDESGPSIVHR
27.52	P60709	2	99	SYELPDGQVITIGNER
27.52	P60709	2	99	TTGIVMDSGDGVTHTVPIYEGYALPH
27.52	P60709	2	99	TTGIVMDSGDGVTHTVPIYEGYALPHAILR
27.52	P60709	2	99	VAPEEHPVLLTEAPLNPK
27.52	P60709	2	99	YPIEHGIVTNWDDMEK
Tubulin α-6 chain				
12.16	P68363	2	99	IHFPLATYAPVISAEK
12.16	P68363	2	99	LISQIVSSITASLR
12.16	P68363	2	99	NLDIERPTYTNLNR
12.16	P68363	2	99	QLFHPEQLITGK
12.16	P68363	2	99	VGINYQPPTVVPGGDLAK
Filamin-A				
2.69	P21333	2	99	ALTQTGGPHVK
Ubiquitin				
6.28	P62988	2	99	TITLEVEPSDTIENVK
6.28	P62988	2	99	TLSDYNIQK
Myosin light polypeptide 6				
5.1	P60660	2	99	VLDFEHFLPMLQTVAK
5.1	P60660	1.7	98	HVLVTLGEK
Glyceraldehyde-3-phosphate dehydrogenase				
15.64	P04406	2	99	GALQNIIPASTGAAK

15.64	P04406	2	99	LISWYDNEFGYSNR
15.64	P04406	2	99	LVINGNPITIFQER
15.64	P04406	2	99	VIHDNFGIVEGLMTTVHAITATQK
15.64	P04406	2	99	VIISAPSADAPMFVMGVNHEK
15.64	P04406	2	99	VPTANVSVVDLTCR
15.64	P04406	2	99	VVDLMAHMASK
Pyruvate kinase isozymes				
8.62	P14618	2	99	APIIAVTR
8.62	P14618	2	99	GVNLPGAAVDLPAVSEK
8.62	P14618	1.7	98	GDYPLEAVR
8.62	P14618	1.7	98	KGVNLPGAAVDLPAVSEK
Peptidyl-prolyl cis-trans isomerase A				
6	P62937	2	99	IIPGFMCQGGDFTR
6	P62937	2	99	SIYGEKFEDENFILK
6	P62937	2	99	VNPTVFFDIAVDGEPLGR
Fructose-bisphosphate aldolase A				
2.53	P04075	2	99	LQSIGTENTEENRR
Annexin A2				
9.33	P07355	2	99	GDLENAFLNLVQCIQNKPLYFADR
9.33	P07355	2	99	GLGTDEDSLIEIICSR
9.33	P07355	2	99	SALSGHLETVILGLLK
Heterogeneous nuclear ribonucleoproteins A2/B1				
7.7	P22626	2	99	EESGKPGAHVTVK
7.7	P22626	2	99	IDTIEIITDR
7.7	P22626	2	99	YHTINGHNAEVR
Eukaryotic translation initiation factor 5A-1				
2	P63241	2	99	VHLVGIDIFTGK
Elongation factor 2				
3.34	P13639	2	99	NMSVIAHVDHGK
Chloride intracellular channel protein 1				
2.3	O00299	2	99	LAALNPESNTAGLDIFAK
40S ribosomal protein S12				
2	P25398	2	99	TALIHDGLAR
ADP/ATP translocase 1				
2.51	P12235	2	99	GNLANVIR
Glucose-6-phosphate isomerase				
2.01	P06744	2	99	ILLANFLAQTEALMR
Protein disulfide-isomerase precursor				
2.26	P07237	1.7	98	SNFAEALAAHK

Thioredoxin (Trx)				
2	P10599	2	99	VGEFSGANK
Talin-1				
6.94	Q9Y490	2	99	ALEATTEHIR
6.94	Q9Y490	2	99	GVGAAATAVTQALNELLQHVK
6.94	Q9Y490	2	99	MVGGIAQIIAAQEEMLR
Ezrin (p81) (Cytovillin)				
6.44	P15311	2	99	FYPEDVAEELIQDITQK
6.44	P15311	2	99	IGFPWSEIR
Filamin-B				
4.53	O75369	2	99	VNIGQGSHPQK
4.53	O75369	2	99	VVASGPGLEHGK
Transgelin				
2.06	Q01995	2	99	KYDEELEER
Histone H2B type F-S				
9.08	P57053	2	99	AMGIMNSFVNDIFER
9.08	P57053	2	99	QVHPDTGISSK
Histone H3.1				
5.58	P68431	2	99	FQSSAVMALQEACEAYLVGLFEDTNLCAIHAK
Eukaryotic translation initiation factor 2C 4				
2.22	Q9HCK5	1.7	98	EVVDTMVRHFK
NHP2-like protein 1				
2	P55769	2	99	AYPLADAHLTK
Ras-related protein Rap-1b				
2	P61224	2	99	INVNEIFYDLVR
Calgizarrin				
3.1	P31949	2	99	TEFLSFMNTELAAFTK

Table 4

(a)

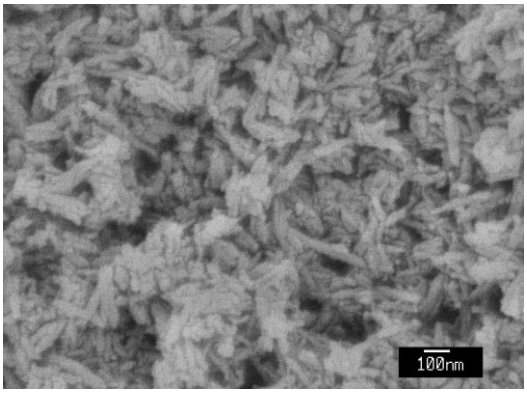

(b)

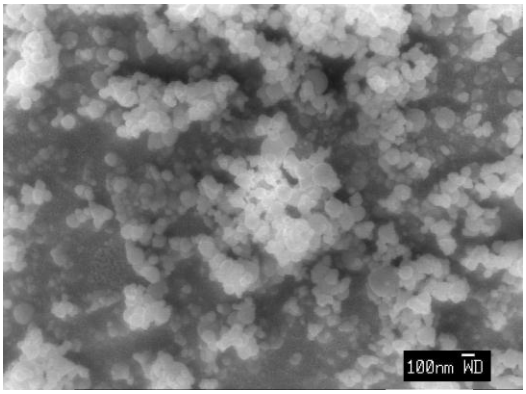

Fig. 1

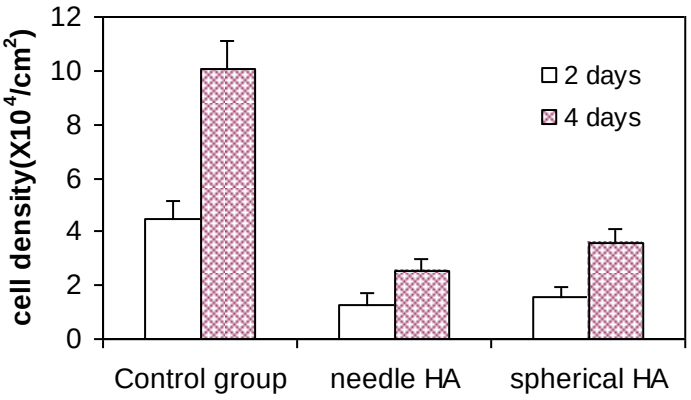
cell density(X10^4/cm^2)
12
10
8
6
4
2
0
2 days
4 days
Control group
needle HA
spherical HA

Fig. 2

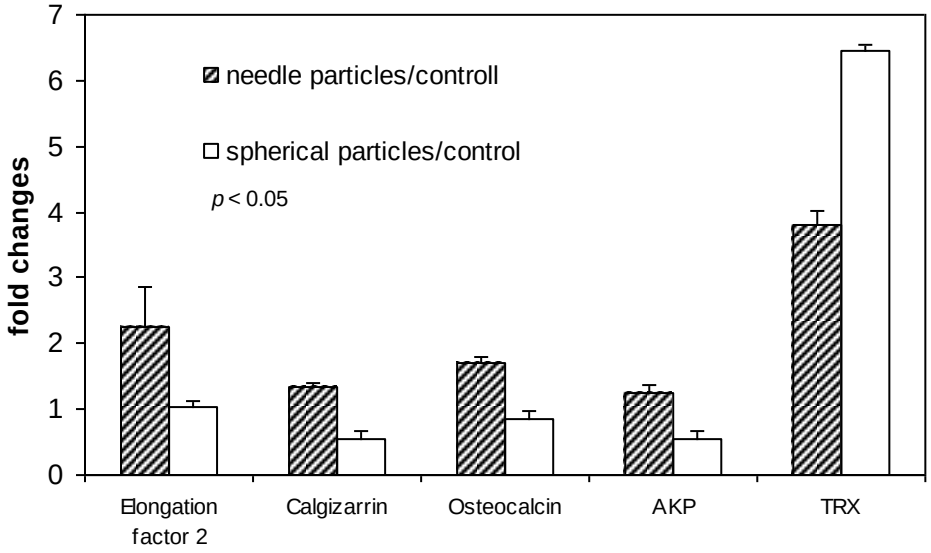
7
6
5
4
3
2
1
0
fold changes
needle particles/controll
spherical particles/control
p < 0.05
Elongation factor 2
Calgizarrin
Osteocalcin
AKP
TRX

Fig. 3